Reprinted from

SENSORS AND ACTUATORS

A PHYSICAL

J31

Sensors and Actuators A 50 (1995) 1–6

Interaction elimination for multicomponent strain-gauge dynamometers

Wenlin Jin [a,*], P.K. Venuvinod [b]

[a] *Mechanical Engineering Department, Nanjing University of Aeronautics and Astronautics, Nanjing 210016, China*
[b] *Manufacturing Engineering Department, City Polytechnic of Hong Kong, 83 Tat Chee Avenue, Hong Kong, Hong Kong*

Received 8 August 1994; in revised form 11 May 1995; accepted 18 May 1995

ELSEVIER

ELSEVIER

Sensors and Actuators A 50 (1995) 1–6

SENSORS AND ACTUATORS A PHYSICAL

Interaction elimination for multicomponent strain-gauge dynamometers

Wenlin Jin [a,*], P.K. Venuvinod [b]

[a] Mechanical Engineering Department, Nanjing University of Aeronautics and Astronautics, Nanjing 210016, China
[b] Manufacturing Engineering Department, City Polytechnic of Hong Kong, 83 Tat Chee Avenue, Hong Kong, Hong Kong

Received 8 August 1994; in revised form 11 May 1995; accepted 18 May 1995

Abstract

A new compensating gauge method has been developed for the elimination of force interactions in multicomponent strain-gauge dynamometers at inner-bridge level so that force components may be read independently from each other. Theoretical analyses as well as verifying experiments have been carried out. Good agreement between theoretical and experimental results is seen and the effectiveness of the new method is verified.

Keywords: Dynamometers; Interaction elimination; Strain gauges

1. Introduction

The outputs of a properly designed strain-gauge multicomponent force sensor are linear functions of the force components:

$$u_i = \sum_{j=1}^{n} k_{ij} f_j \tag{1}$$

or in a matrix form

$$\mathbf{U} = \mathbf{KF} \tag{2}$$

Ideally, **K** should be a diagonal matrix, which means the sensor is interaction-free and force components may be directly read or used for feedback controlling purpose. However, by reviewing the present literature it may be found that because of unavoidable manufacturing errors, it is very difficult, if not impossible, to eliminate the interaction in common designs even if very sophisticated structures are adopted [1]. It has been a common practice that force components are calculated from the outputs using the inverse matrix $\mathbf{A} = \mathbf{K}^{-1}$ [2–7]:

$$\mathbf{F} = \mathbf{AU} \tag{3}$$

or

$$f_j = \sum_{i=1}^{m} a_{ji} u_i \quad j = 1, 2, \ldots, n \tag{4}$$

The calculation defined by Eqs. (3) or (4) may be done by a modern computer within an extremely short time or by a specially designed signal-processing circuit [8]. However, it should be noticed that both hardware and software methods belong to data-processing techniques rather than improvements of the performance of sensors and, what is more important, fulfilling the calculation is based on the whole set of sensor outputs $\{u_i\}$ (see Eq. (4)). If one or several components of $\{u_i\}$ are unavailable due to certain particular restrictions, for example, restrictions from fabrication techniques to micro-force-sensor development [9] and structure restrictions to some special kinds of force-sensor development [10], the calculation cannot be done.

With a view to eliminating the interactions of each bridge independently, we have developed a new method, the compensating-gauge method, which is described here.

2. The principle of the compensating-gauge method

Fig. 1 shows the principle of the compensating-gauge method. f_i are interacting force components and B_j is the

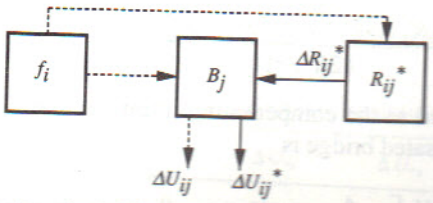

Fig. 1. Illustration of principle of the compensating gauge method $i = 1$–n, $i \neq j$.

* Corresponding author. Present address: Department of Mechanical Engineering, University of California, 6189 Etchverry Hall #1740, Berkeley, CA 94720-1740, USA.

SSDI 0924-4247(95)01033-W

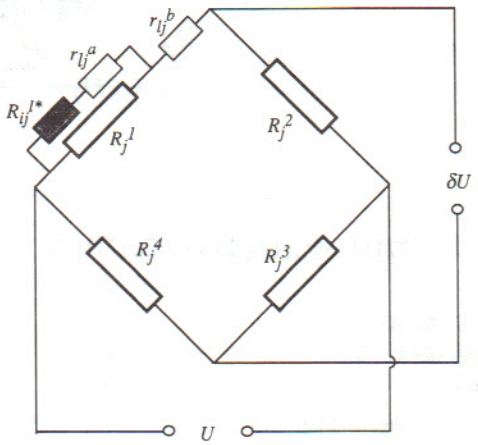

Fig. 2. Incorporation of compensating gauge in a measuring bridge.

measuring bridge for the jth force component f_j. Under the ith interacting force component f_i, B_j will yield an interaction output ΔU_{ij} as shown in the Figure. To eliminate ΔU_{ij}, a compensating gauge R_{ij}^*, the output of which is designed to be sensitive to f_i, is incorporated into B_j. The resistance increment of the compensating gauge due to f_i, ΔR_{ij}^*, will then cause a corresponding output of the bridge, ΔU_{ij}^*. If ΔU_{ij}^* is made in such a way that its sign is opposite to, and its magnitude the same as that of ΔU_{ij}, the interaction output will be fully offset at inner-bridge level.

Fig. 2 shows the manner in which the compensating gauge ΔR_{ij}^{l*} is incorporated into the jth bridge, B_j, where R_j^1–R_j^4 are arm gauges, r_{ij}^a is a constant resistance, the function of which is to adjust the intensity of the compensation, and r_{ij}^b is another constant resistance, the function of which is to keep the compensated bridge in a balanced state when the sensor is load-free. The subscript l indicates the number of the arm in which the compensating gauge is located (here $l=1$). The resistance increment of the compensated arm due to f_i is (for derivation, see Appendix A):

$$\delta R_{ij}^l = \left(\frac{R}{2R+r_{lj}^a}\right)^2 \Delta R_{ij}^{l*} + \left(\frac{R+r_{lj}^a}{2R+r_{lj}^a}\right)^2 \Delta R_{ij}^l \tag{5}$$

where ΔR_{ij}^{l*} and ΔR_{ij}^l are resistance increments of R_{ij}^{l*} and R_{ij}^l, respectively, and R is the magnitude of the resistance of the gauges. Rearranging Eq. (5), we have

$$\delta R_{ij}^l = (1+X_{ij}^l)\Delta R_{ij}^l \tag{6}$$

where

$$X_{ij}^l = \frac{(\Delta R_{ij}^{l*}/\Delta R_{ij}^l)R^2 - (3R+2r_{lj}^a)R}{(2R+r_{lj}^a)^2} \tag{7}$$

is defined at the compensating intensity. The output of the compensated bridge is

$$\delta U_{ij} = \frac{U}{4R}\left[\sum_{k=1,\,k\neq l}^{4}(-1)^{k-1}\Delta R_{ij}^k + (-1)^{l-1}\delta R_{ij}^l\right] \tag{8}$$

Substituting Eq. (6) into Eq. (8), we can separate the compensated output into two parts, the original output and the compensating output, as shown by the following equation:

$$\delta U_{ij} = \frac{U}{4R}\sum_{k=1}^{4}(-1)^{k-1}\Delta R_{ij}^k + \frac{U}{4R}(-1)^{l-1}X_{ij}^l\Delta R_{ij}^l$$
$$= \Delta U_{ij} + \Delta U_{ij}^l \tag{9}$$

When there is more than one interaction force component, more compensating gauges should be introduced to eliminate all the interaction outputs. Following the above procedure, we can derive the expressions for outputs of a compensated bridge, in which n-1 compensating gauges are introduced into its different arms, due to the interacting force components f_i:

$$\delta U_{ij} = \frac{U}{4R}\left[\sum_{k=1}^{4}(-1)^{k-1}\Delta R_{ij}^k + \sum_{l=l_1}^{l_{n-1}}(-1)^{l-1}X_{ij}^l\Delta R_{ij}^l\right]$$
$$= \Delta U_{ij} + \sum_{l=l_1}^{l_{n-1}}\Delta U_{ij}^l \tag{10}$$

Letting $\delta U_{ij}=0$, we have

$$\sum_{k=1}^{4}(-1)^{k-1}\Delta R_{ij}^k + \sum_{l=l_1}^{l_{n-1}}(-1)^{l-1}X_{ij}^l\Delta R_{ij}^l = 0 \tag{11}$$

$$i = 1\text{–}n,\ j\neq i$$

Substituting Eq. (7) into Eq. (11), we obtain an $n-1$ dimensional non-linear equation set with $n-1$ adjusting resistances as the unknowns. The solution of the equation set yields $n-1$ adjusting resistances r_{ij}^{a*}. The magnitudes of corresponding balance resistances may then be calculated according to

$$r_{ij}^b = \frac{R^2}{2R+r_{ij}^b} \tag{12}$$

so that the compensated arm resistance is kept equal to R when the sensor is load-free.

3. Discussion

3.1. A simple way of implementing the method

As has been noted above, the implementation of the new method involves the problem of solving a multivariable non-linear equation set. It is commonly known that, with few exceptions, a direct solution of a non-linear equation set is impossible. When numerical methods are used it is usually not easy to discuss or examine the convergence of the solution [11]. This problem could become a hindrance in the application of the new method.

However, it may be seen from Eq. (7) that, if the ratios of the resistance increments of a specific compensating gauge, $\alpha_{ij}^l = \Delta R_{ij}^{l*}/\Delta R_{ij}^l$, under different interaction force components are the same, the compensating intensity will be independent of the index i. Taking $n-1$ compensating intensities as the unknowns, we can first solve equation set (11), which is

linear, to obtain $n-1$ *expected* compensating intensities, X_{ij}^{l*}, and then calculate the corresponding $n-1$ adjusting resistances, r_{ij}^{a*}, from Eq. (7). Thus, the problem of solving a nonlinear equation set is avoided.

In practice, the simplest way of making the resistance increment ratios α_{ij}^{l} equal is taking a constant resistance of magnitude R to replace the compensating gauge. In such a way all the ratios α_{ij}^{l}, $i=1$–n, are the same and equal to zero. The compensating intensity is then only dependent on r_{ij}^{a} as shown by the following equation:

$$X_j^l = -\frac{(3R+2r_{lj}^a)R}{(2R+r_{lj}^a)^2} \tag{13}$$

Conversely, when the expected compensating intensity X_{ij}^{l*} is known, the corresponding adjusting resistance is given by

$$r_{lj}^{a*} = \frac{-(2X_j^{l*}+1)-(1+X_j^{l*})^{1/2}}{X_j^{l*}} \tag{14}$$

Besides simplicity in calculation, another advantage of this simple implementation is that no compensating gauges are required. This will be very important when a compact sensor is to be developed where there is inadequate room for the gauges.

3.2. Influence of compensating gauge on bridge sensitivity

Evidently incorporation of compensating gauges into a bridge, B_j, will also influence its output due to the jth force component f_j. Following Eqs. (10) and (7), we have

$$\delta U_{jj} = \frac{U}{4R}\left[\sum_{k=1}^{4}(-1)^{k-1}\Delta R_{jj}^k + \sum_{l=l_1}^{l_{n-1}}(-1)^l X_{jj}^l \Delta R_{jj}^l\right]$$
$$= \Delta U_{jj} + \sum_{l=l_1}^{l_{n-1}} \Delta U_{jj}^l \tag{15}$$

where

$$X_{jj}^l = \frac{(\Delta R_{jj}^{l*}/\Delta R_{jj}^l)R^2 - (3R+2r_{ij}^a)R}{(2R+r_{ij}^a)^2} \tag{16}$$

From these equations, we can see that the additional output due to the introduction of the compensating gauges $\Sigma\Delta U_{jj}^l$ may be determined when the magnitude of the adjusting resistance r_{ij}^a and the ratio $\alpha_{jj}^l = \Delta R_{jj}^{l*}/\Delta R_{ij}^l$ are known.

Defining $\lambda_j^l = \Delta U_{jj}^l/\Delta U_{jj}$ as the *sensitivity attenuation coefficient*, we have

$$\lambda_j^l = \frac{(-1)^{l-1}X_{jj}^l \Delta R_{jj}^l}{\sum_{k=1}^{4}(-1)^{k-1}\Delta R_{jj}^k} \tag{17}$$

and

$$\delta U_{jj} = \left(1+\sum_{l=l_1}^{l_{n-1}}\lambda_j^l\right)\Delta U_{jj} \tag{18}$$

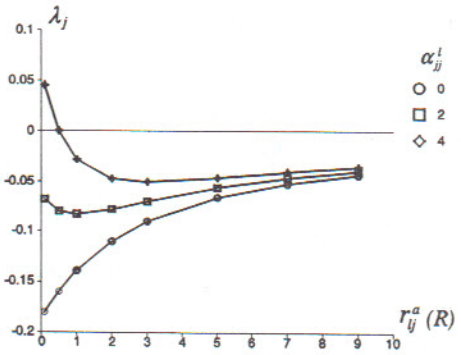

Fig. 3. Dependence of sensitivity attenuation coefficient on adjusting resistance.

Suppose that the contributions of the resistance increments of four arm gauges to the output are the same, that is,

$$(-1)^{l-1}\Delta R_{jj}^l = \frac{1}{4}\sum_{k=1}^{4}(-1)^{k-1}\Delta R_{jj}^k \tag{19}$$

we can plot λ_j^l against r_{ij}^a and the ratio α_{jj}^l as shown in Fig. 3. It is apparent that, with the same r_{ij}^a, a larger value of α_{jj}^l corresponds to a lower sensitivity attenuation and the effect of α_{jj}^l on λ_j^l is remarkably significant when the value of r_{ij}^a is small. Therefore r_{ij}^a and α_{ij}^l should be made large in designing the compensating gauge.

4. Experimental verification

A three-component turning sensor was designed to verify the above concepts (see Appendix B). Each measuring bridge was composed of four arm gauges. Six compensating gauges were also designed for later use. Constant load (300 N dead weights) were applied to the sensor in the three directions of F_x, F_y, F_z, which are perpendicular to each other and represent the feed, thrust and cutting force components, respectively. The outputs from the three original measuring bridges were recorded and are listed in Table 1. It can be seen

Table 1
Original outputs from the measuring bridges. Excitation input voltage to the bridges, $U=5$ V

Applied load (N)			Output of measuring bridge (μV)		
F_x	F_y	F_z	ΔU_{*x}	ΔU_{*y}	ΔU_{*z}
300	0	0	180.4	3.2	5.0
0	300	0	2.1	112.1	3.2
0	0	300	−5.4	−3.2	165.7

that the interactions are of the order of 2–3%, which could lead to measuring errors as high as 5% if they are not controlled.

For the purpose of compensating the interaction outputs using the new method, the resistance increments of all the twelve arm gauges as well as the six compensating gauges were measured under the same experimental conditions. The data were analysed and the locations of the six compensating gauges were determined. Table 2 lists the results.

Substituting the data from Table 2 into Eqs. (7) and (11), we obtain three two-dimensional non-linear equation sets. A numerical method was developed for the solution of the equation sets so that the magnitudes of the six adjusting resistances are obtained as listed in Table 3. After the adjusting resistances were determined, the sensitivity attenuation coefficients for each compensating gauge, and consequently the compensated outputs of the bridges, were calculated. The calibration of the compensated sensor was done to verify the calculated results. Table 3 compares the results from the calculations with those from the experiments.

Experiments were also carried out to verify the simple implementation of the new method. Three linear equation sets were established by substituting the data from Table 2 into Eq. (11), and the six expected compensating intensities were obtained by solving these equation sets. Corresponding adjusting resistances were then calculated from Eq. (14). The compensated outputs were consequently calculated from Eqs. (10) and (15). Table 4 lists the calculated results and the measured outputs of the bridges compensated in this simple way under the same experimental condition as described above. From Tables 3 and 4 we can see that:

(a) in both cases the calculated and measured results are quite close (this verifies the correctness of the equations derived in this paper);

(b) all the interaction outputs are greatly reduced and the sensitivity reduction is slight (the effectiveness of the new method is thus verified);

(c) when the compensating gauges are used, the sensitivity reduction is less than that when the compensating gauges are replaced with constant resistances.

Table 2
Resistance increments of all gauges and the locations of compensating gauges (original resistance of strain gauges, $R = 350\ \Omega$)

Load	Resistance increments ($10^{-4}\ \Omega$)																					
	ΔR_x^1	ΔR_x^2	ΔR_x^3	ΔR_x^4	ΔR_{yx}^*	ΔR_{zx}^*	ΔR_y^1	ΔR_y^2	ΔR_y^3	ΔR_y^4	ΔR_{xy}^*	ΔR_{zy}^*	ΔR_z^1	ΔR_z^2	ΔR_z^3	ΔR_z^4	ΔR_{xz}^*	ΔR_{yz}^*
F_x	124	−130	128	−123	−128	120	53	48	−51	−52	121	−110	104	115	−112	−108	−130	110
F_y	−88	−90	−84	−91	87	−85	87	−79	90	−86	−83	86	−86	−82	−82	−77	−85	−92
F_z	117	112	−109	−117	123	−124	−58	50	58	−59	115	−109	118	−120	109	−117	−117	108
					$l=4$	$l=1$					$l=4$	$l=3$					$l=2$	$l=3$

5. Conclusions

Both the theoretical and experimental results show that the compensating-gauge method proposed in this paper provides an effective way to eliminate the interaction outputs of a multicomponent strain-gauge sensor at the inner-bridge level without requiring complex structural design and high manufacturing precision.

There are two ways of implementing the proposed method. The first is characterized by lower sensitivity attenuation but at the expense of a relatively complex calculation procedure. The second is simple in calculation but its sensitivity attenuation is relatively greater.

Table 3
Calculated and measured compensating results: part one (c: calculated; m: measured)

	Adjusting resistance (Ω)			Sensitivity attenuation coefficient (%)		Compensated output (μV)					
	r^a_{*x}	r^a_{*y}	r^a_{*z}	$\Sigma\lambda^l_*$		dU_{*x}		dU_{*y}		dU_{*z}	
				c	m	c	m	c	m	c	m
B_x		5974	11439	−2.567	−2.772	175.7	175.4	0	0.02	0	0.11
B_y	4719		34279	−3.564	−3.849	0	0	117.8	117.4	0	−0.13
B_z	88974	4856		−2.975	−3.078	0	0.01	0	0.06	160.8	160.6

Table 4
Calculated and measured compensating results: part 2

	Expected compensating intensity			Adjusting resistance (Ω)			Compensated output (μV)					
	X^{l*}_{*x}	X^{l*}_{*y}	X^{l*}_{*z}	r^{a*}_{*z}	r^{a*}_{*y}	r^{a*}_{*z}	δU_{*x}		δU_{*y}		δU_{*z}	
							c	m	c	m	c	m
B_x		−0.1086	−0.0101		5563	68567	175.1	174.6	0	−0.10	0	0.9
B_y	−0.1339		−0.0189	4345		36120	0	0.08	117.4	117.2	0	−0.10
B_z	−0.0119	−0.1217		57817	4872		0	0.05	0	−0.03	160.4	160.1

Appendix A

Let

$$r = R + r^a_{ij} \tag{A1}$$

The original resistance of the arm is

$$R^l_0 = \frac{Rr}{R+r} \tag{A2}$$

The resistance of the arm when f_i is applied is

$$R^l_i = \frac{(R+\Delta R^l_{ij})(r+\Delta R^{l*}_{ij})}{R+\Delta R^l_{ij}+r+\Delta R^{l*}_{ij}} \tag{A3}$$

The resistance increment is than

$$\begin{aligned}\delta R^l_{ij} &= \frac{(R+\Delta R^l_{ij})(r+\Delta R^{l*}_{ij})}{R+\Delta R^l_{ij}+r+\Delta R^{l*}_{ij}} - \frac{Rr}{R+r} \\ &= \frac{1}{R+\Delta R^l_{ij}+r+\Delta R^{l*}_{ij}} \\ &\quad \times \left[R\Delta R^{l*}_{ij} + r\Delta R^l_{ij} + \Delta R^{l*}_{ij}\Delta R^l_{ij} - \frac{Rr}{R+r}(\Delta R^{l*}_{ij} + \Delta R^l_{ij}) \right] \\ &= \frac{1}{R+\Delta R^l_{ij}+r+\Delta R^{l*}_{ij}} \\ &\quad \times \left[\frac{R^2}{R+r}\Delta R^{l*}_{ij} + \frac{r^2}{R+r}\Delta R^l_{ij} + \Delta R^{l*}_{ij}\Delta R^l_{ij} \right]\end{aligned} \tag{A4}$$

Considering the fact that ΔR^{l*}_{ij} and ΔR^l_{ij} are much smaller than R, we have

$$\delta R^l_{ij} = \left(\frac{R}{R+r}\right)^2 \Delta R^{l*}_{ij} + \left(\frac{r}{R+r}\right)^2 \Delta R^l_{ij} \tag{A5}$$

Substituting Eq. (A1) into Eq. (A5) yields Eqn. (5).

Appendix B

As shown in Fig. B1, four shear panels are used as main elastic elements. Shear strains induced by f_x and f_z on the panels are detected as the measurements of corresponding

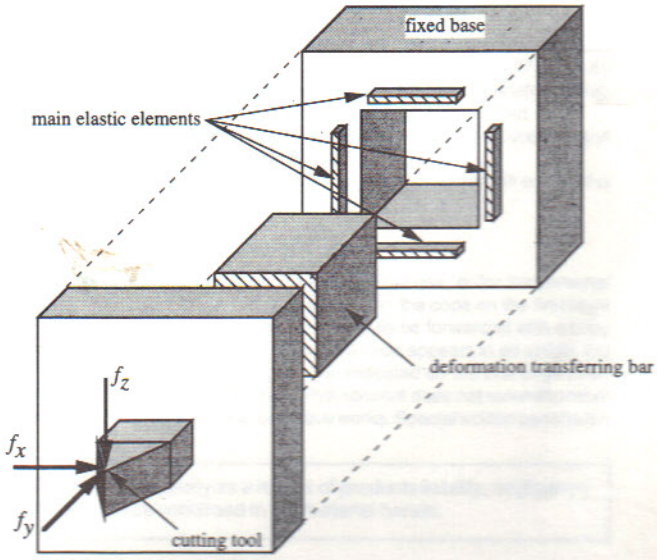

Fig. B1. General view of the design of the cutting dynamometer.

force components. A pair of *secondary elastic elements* with very low stiffness is designed between the deformation transferring bar and the fixed base to convert the deformation of the main elements in the y direction due to f_y into shear strains, which are then detected as the measurement of f_y. Compensating gauges R_{xz}, R_{xy}, R_{zx} and R_{zy} are located on the main elements and R_{yz} and R_{yx} are on the *secondary elements*.

References

[1] Y. Nukamura, T. Yoshikawa and I. Futamata, Design and signal processing of six-axis force sensor, in C. Roberts and B. Roth (eds.), *Robotics Research,* MIT Press, Boston, MA, 1985, pp. 75–81.

[2] S.E. Oraby, High-capacity compact three-component cutting force sensor, *Int. J. Mach. Tools Manuf., 30* (1990) 549–554.

[3] M. Uchiyama, E. Bayo and E. Palma-Villalon, Systematic design procedure to minimize the performance index for robot force sensors, *J. Dynamic Syst., Measurement Control, Trans. ASME, 113* (1991) 388–394.

[4] H. van Brussel, H. Belien and H. Thielemans, Force sensing for advanced robot control, *Proc. 5th Int. Conf. Robot Vision Sensory Controls,* IFS Publications, Amsterdam, 1985, pp. 59–68.

[5] M. Dubois, Six-component strain-gauge balances for large wind tunnels, *Exp. Mech., 21* (1981) 401–407.

[6] C.T. Lin and C.W. Beadle, The optimal design of force transducers which are cross-axis sensitive, in K.A. Stetson and L.M. Sweet (eds.), *Sensors and Controls for Automated Manufacturing and Robotics,* ASME, New York, 1984, pp. 179–191.

[7] S.A. Masroor and L.W. Zachary, Designing an all purpose force transducer, *Exp. Mech., 31* (1991) 33–36.

[8] Reports of Scientific & Technical Committee of CIRP: recommendation for the calibration and operation of machine tool dynamometers, *Ann. CIRP, 23* (1974) 295–306.

[9] J. Shajii, K. Ng and M.A. Schmidt, A microfabricated floating-element shear stress sensor using wafer bonding technology, *J. Microelectromech. Syst., 1* (1992) 889–904.

[10] H. Zheng, Studies on measurement of forces acting on machine tool spindles, *Degree Dissertation,* Nanjing University of Aeronautics and Astronautics, China, Feb. 1994 (in Chinese).

[11] G.D. Byrne, *Numerical Solution of Systems of Nonlinear Algebraic Equations,* Academic Press, New York, 1973.

Biographies

Wenlin Jin graduated from Hefei Polytechnic University, China with a B.S. degree in 1982. He received the Ph.D. degree in mechanical engineering at Nanjing University of Aeronautics and Astronautics, China, and joined the faculty of the same university in 1988. Between 1988 and 1992 his main research area included machining process monitoring and optimization and multicomponent dynamic force sensors. From July 1992 to June 1993 he worked in the City Polytechnic of Hong Kong as a visiting scholar. Since July 1993 he has been a professor at the Nanjing University of Aeronautics and Astronautics. He is now visiting the University of California at Berkeley, USA, working on microsensors.

Patri K. Venuvinod obtained his first degree in mechanical engineering from Osmania University, India, in 1963 and a Ph.D. degree from the University of Manchester, UK. In the period 1965 to 1978, he worked as a lecturer and associate professor at the Regional Engineering College, Warangal, India. In the period 1978 to 1987, he worked as a senior lecturer and principle lecturer at Hong Kong Polytechnic. In 1987 he was appointed as the funding chairman and professor of the Department of Manufacturing Engineering, City Polytechnic of Hong Kong. He is a fellow of the Institution of Electrical Engineers (UK), an associate member of ASME and a senior member of IIE. His current research interests include modelling of metal cutting operations, chip control, design for assembly, feature recognition, artificial neural nets and condition monitoring of machine tools.